

1 **Liquidus Tracking:**  
2 **Large scale preservation of encapsulated**  
3 **3-D cell cultures using a vitrification machine**

4 Eva Puschmann<sup>a\*</sup>, Clare Selden<sup>a</sup>, Steve Butler<sup>b</sup> and Barry Fuller<sup>c</sup>

5 <sup>a</sup>UCL, Institute for Liver & Digestive Health, Royal Free Campus, London, NW3 2PF, UK

6 <sup>b</sup>Planer PLC, 110 Windmill Road, Sunbury-on-Thames, UK

7 <sup>c</sup>UCL, Department of Surgery, Royal Free Campus, London, NW3 2PF, U.K.

8 <sup>\*</sup>For correspondence: [eva.puschmann.10@ucl.ac.uk](mailto:eva.puschmann.10@ucl.ac.uk)

9

10 **Abstract**

11 Currently, cryo-banking of multicellular structures such as organoids, especially in large  
12 volumes at clinical scale >1 litre, ~~and large volumes~~ remains elusive for reasons such as  
13 insufficient dehydration and cryoprotectant additive (CPA<sup>1</sup>) penetration, slow cooling and  
14 warming rates and devitrification processes. Here we introduce the concept of Liquidus  
15 Tracking (LT) using a semi-automated device for liquid volumes of up to 450ml including  
16 130ml of alginate encapsulated liver cells (AELC) that archived controlled and reversible  
17 vitrification with minimized toxicity.  
18 First a CPA solution with optimal properties for LT was developed by employing different  
19 small scale test systems. Combining sugars such as glucose and raffinose with Me<sub>2</sub>SO  
20 improved post-exposure (at +0.5°C) viabilities from 6 +/- 3.6% for Me<sub>2</sub>SO alone up to 58 +/-  
21 6.1% and 65 +/- 14.2 % respectively (p<0.01). Other permeating CPAs (e.g. ethylene glycol,  
22 propylene glycol, methanol) were investigated as partial replacements for Me<sub>2</sub>SO. A mixture

---

<sup>1</sup> cryoprotectant additive (CPA), Liquidus Tracking (LT), alginate encapsulated liver cells (AELC), alpha-fetoprotein (AFP), mixture of Me<sub>2</sub>SO, ethylene glycol and glucose (ratio 4:2:1): termed LTdeg.

23 of Me<sub>2</sub>SO, ethylene glycol and glucose (ratio 4:2:1– termed LTdeg) supported glass-forming  
24 tendencies with appropriate low viscosities and toxicities required for LT. When running the  
25 full LT process, using Me<sub>2</sub>SO alone, no viable cells were recovered; using LTdeg, viable  
26 recoveries were improved to 40+/-8% (p<0.001%). Further refinements of improved mixing  
27 technique further improved recovery after LT. Recoveries of specific liver cell functions such  
28 as synthesis of albumin and alpha-fetoprotein (AFP) were retained in post thaw cultures.  
29 In summary: By developing a low-toxicity CPA solution of low viscosity (LTdeg) suitable  
30 for LT and by improving the stirring system, post-warming viability of AELC of up to 90%  
31 and a AFP secretion of 89% were reached. Results show that it may be possible to develop  
32 LT as a suitable cryogenic preservation process for different cell therapy products at large  
33 scale.

#### 34 **Keywords**

35 Liquidus Tracking, large volume vitrification, CPA toxicity, Bioartificial liver device

#### 36 **Introduction**

37 Scientists have successfully cryopreserved a variety of cells over the last 40 years, but success  
38 has mainly been achieved by traditional slow cooling with cell suspensions in small (<10 ml)  
39 volumes [16,45] in tube format, or in bag format in volumes of up to 200ml [10,17,33].  
40 Cooling multicellular systems down to deep sub-zero temperatures has proven far more  
41 challenging, especially when large volumes of biomass require cryo-banking. These problems  
42 began to be understood during early attempts to cryopreserve whole organs or large complex  
43 tissues. They were mainly related to the formation of extracellular ice in liquid spaces within  
44 the tissue [37], such as within small capillary blood vessels inside an organ [19], which  
45 physically destroyed the internal structure. In addition, disruptive ice propagation between  
46 inter-connected cells [1], insufficient cell dehydration and CPA penetration during slow  
47 cooling and ice-recrystallization during the warming process have all been noted. These can

48 also make cell agglomerates more susceptible to freezing damage than individual cells. Ice  
49 formation can be avoided by vitrification, but high cooling rates must frequently be imposed  
50 to avoid toxic effects from the essentially high CPA concentrations required and to maximise  
51 the likelihood of achieving the glassy state without ice nucleation events [13]. This remains a  
52 significant challenge for large tissues or, equally, for large volumes of functionally  
53 interconnected cells such as cell spheroids, as enough time must be given for CPA to  
54 penetrate into the all the cells, including those in the core, and for the core cells to dehydrate  
55 sufficiently to avoid intracellular freezing, risking toxic effects during CPA exposure and  
56 cooling. CPA toxicity is also critical during the warming process when high concentrations of  
57 CPAs will be present when the cryogenic glasses begin to liquefy; equally the high warming  
58 rates needed to prevent devitrification and ice re-crystallisation for all cells within a sample  
59 are difficult to achieve in large volumes [6,7].

60 Many of those obstacles can be overcome by Liquidus Tracking (LT), a method of achieving  
61 vitrification in an aqueous mixture by incrementally increasing concentrations of penetrating  
62 CPAs (up to 70%) at incrementally decreasing temperatures [15,38,47]. Cryoprotectants are  
63 known to be less toxic at lower concentrations, but also at lower temperatures [34,48] due to  
64 decreased cell activity, reduced chemical interaction with sensitive biomolecules and  
65 reduced CPA permeation. Due to reduced CPA toxicity, and avoidance of ice nucleation in  
66 LT, large samples can be vitrified without the necessity of fast cooling rates, or when longer  
67 exposure times are required to allow for sufficient CPA penetration - for example for organ  
68 and tissue vitrification.

69 We have previously studied cryopreservation by slow cooling of alginate encapsulated  
70 multicellular liver cell spheroids (AELC) in developing a bioartificial liver support system  
71 [31]. Treatment volumes of between 1-2 litres of AELC for use in a bioartificial liver device  
72 have been used in our pre-clinical studies [11] and are predicted to be needed for patient

73 therapy. We have also shown that LT vitrification can be applied to AELC in a small volume  
74 feasibility study [40]. Our aim here was to develop a LT protocol, which would allow the  
75 cryo-banking and warming of large volumes of AELC whilst maintaining good functional  
76 recovery. To improve cell viability we have developed a low-toxicity CPA solution for LT  
77 with the requirement of low viscosity (but which – nevertheless – could suppress ice  
78 nucleation) so that it may be used within the Liquidus Tracker equipment. Additionally the  
79 development of a new stirring system substantially increased post-warming viability.

## 80 **Materials and Methods**

81 Unless otherwise stated, all chemicals were sourced from Sigma (Poole, United Kingdom)  
82 and for cooling and warming a PlanerLiquidus Tracker Controller and a Controlled Rate  
83 Freezer (Planer, Kryo 10, Series II chamber) was used. CPA concentrations were used and  
84 reported in weight per volume (w/v) throughout this work.

## 85 **Cell culture and encapsulation**

86 The techniques for culturing HepG2 cells and producing AELC have been described  
87 previously in detail [11]. In brief: Confluent HepG2 monolayer cells (from ECACC,  
88 Wiltshire, UK) were encapsulated into 1% alginate (alginic acid sodium salt *Macrocystis*  
89 *pyrifera* kelp) by calcium-related polymerisation and cultured for >11 days until containing  
90 several thousand cells in spheroids within each alginate bead (average diameter 450µm).

## 91 **Cell culture to different end cell densities**

92 For experiments that required different cell densities, AELC were cultured for either 3, 5, 7, 9  
93 or 11 days before being used for LT.

## 94 **Viability assay**

95 Cell viability was measured by dual staining with fluorescein diacetate and propidium iodide  
96 using an established imaging software method for quantification which has been established

97 against cell number and protein production [21]. Viability was measured after 24 hours post-  
98 treatment, the time point of lowest viability before on-set of recovery [31].

### 99 **Quantification of cell numbers**

100 Cell number quantification using the Nucleoview System (Sartorius Stedim, Epsom, United  
101 Kingdom) has been described previously in detail [11]. Viable cell numbers were calculated  
102 by multiplying the cell number by the viability for each sample.

### 103 **Functional assays to assess protein synthesis by alpha-fetoprotein and albumin secretion**

104 Alpha-fetoprotein (AFP) and albumin synthesis and secretion were measured by sandwich  
105 enzyme-linked immunosorbent assay which has been described previously in detail [11].

### 106 **Viscosity assessment and measurement**

107 Viscosity of CPA mixtures is an important factor in applying LT to facilitate good mixing  
108 and ensure uniform high CPA concentrations to avoid ice nucleation. Viscosity of CPA  
109 solutions was assessed for applicability by comparing new CPA solutions against a reference  
110 solution (70% (w/v) Me<sub>2</sub>SO) by observational grading of resistance to pipetting or to  
111 manually stirring the solution at -40°C – the lowest workable LT temperature from previous  
112 experience [40]. For pipetting a standard 1ml Eppendorf pipette and 1ml pipette tips and for  
113 stirring a stainless steel spatula with a 4mm width were used. 10ml CPA in 15ml Centrifuge  
114 tubes (Falcon, Fisher Scientific) were cooled to -40°C. This test was developed as no  
115 viscometers or rheometers operable at -40°C were available locally and it also allowed direct  
116 rapid assessment of multiple samples. Viscosity was rated 1-4 (1 = similar to 70% (w/v)  
117 Me<sub>2</sub>SO, easy to pipette; 2 = pipetting not possible but can be easily stirred, 3 = very viscous,  
118 stirring very difficult, 4 = stirring not possible, almost a solid). Solutions with a viscosity  
119 rating of “2” were modified by replacing 10% of the highly viscous CPAs with less viscous  
120 CPAs. In particular methanol was selected as a low viscosity CPA to reduce the overall  
121 viscosity of the mixture. Thereafter, viscosities of the most promising CPA solutions were

122 measured at 20°C using a Bohlin CVO automated shear rheometer to provide a set of  
123 reference data. Shear stress ( $s^{-1}$ ) was increased by 10rpm every 10 seconds, from 10 to  
124 250rpm.

### 125 **CPA toxicity tests**

126 A two-step protocol was used to reduce potential CPA-related osmotic injury based on  
127 previous experience with AELC which have shown high viabilities after one step addition  
128 and dilution of up to 40% Me<sub>2</sub>SO (v/v) [40]. A volume of 0.25ml settled beads (AELC) was  
129 incubated in a 30% (w/v) CPA solution for five minutes at room temperature (Falcon tubes,  
130 Fisher Scientific), then for five minutes at 0.5°C (tubes in ice-water). The concentration was  
131 then increased to 60% (w/v) CPA and beads incubated for 10 or 20 minutes at 0.5°C. CPA  
132 concentration and incubation time were chosen to display strong difference in survival  
133 between solutions. By adding 1xPBS for dilution steps, the CPA concentration was reduced  
134 to 30% (w/v). Samples were left on ice for five minutes. Beads were washed twice with 4ml  
135 of 1xPBS and incubated in complete medium for 24 hours before viability was assessed.

### 136 **Optical vitrification assessment**

137 A volume of 4ml of each newly developed CPA solution and Me<sub>2</sub>SO at a concentration of  
138 60% and 70% (w/v) was vitrified in a 12-well plate by cooling samples at -10°C/min to -  
139 160°C. All solutions were then left at room temperature for warming and optical observation.

### 140 **Standard small volume vitrification protocol**

141 A traditional two-step small volume protocol was used to assess vitrification of AELC *per se*  
142 and allow comparison to LT. Therefore 0.25ml settled beads were incubated in a 31.5% (w/v)  
143 CPA solution in Nunc cryo-tubes (1.8 ml, Nunc, Loughborough, UK), first for five minutes at  
144 room temperature and then for an additional five minutes at 0.5°C (tubes in ice-water). The  
145 CPA concentration was increased to 63% (w/v) using a 70% (w/v) pre-cooled CPA solution  
146 (at 0.5°C). Samples were left on ice for five minutes and then plunged into liquid nitrogen.

147 Samples were warmed for approximately eight minutes on ice until they reached a liquid  
148 state. By adding ice cold 1xPBS (+Mg<sup>2+</sup>, Ca<sup>2+</sup>) the CPA concentration was reduced to 31.5%  
149 (w/v). Samples were left on ice for five minutes before washing twice with 4ml 1xPBS  
150 (+Mg<sup>2+</sup>, Ca<sup>2+</sup>). Finally, AELC were incubated in complete media for 24 hours before  
151 assessing viability.

## 152 **Liquidus Tracking**

153 The prototype Planer LT machine consists of a sample carrier with a magnetic stirrer which is  
154 placed inside a Controlled Rate Freezer (Planer, Kryo 10, Series II chamber) and an inlet and  
155 outlet pump system [40]. All of these units are connected to a controller, which allows a  
156 completely automated cooling, mixing and addition and extraction process when using a single  
157 highly concentrated CPA solution. For the work presented here the peristaltic pumps were  
158 operated manually to allow for the use of differently concentrated CPA inlet solutions for  
159 both the cooling and warming process. A liquid volume of 450ml including 130ml of settled  
160 beads was used for each run, if not stated otherwise.

161 (i) LT cooling: The controlled rate freezer was first set on hold at -20°C and then -25°C until  
162 the sample reached a concentration of 32% (w/v) at -12°C and 40% (w/v) at -16°C,  
163 respectively, by pumping in a 50% CPA inlet solution. After that the freezer was set to -  
164 30°C and a 60% (w/v) CPA solution was used to increase the sample to 50% (w/v) (at -  
165 20°C) and subsequently a 66% (w/v) CPA solution was added to reach a final sample  
166 concentration of 64% (w/v) (at -20°C). CPA increase to 25% (w/v) were carried out by  
167 addition only, increase to 64% (w/v) was reached by operating both inlet and outlet  
168 pump simultaneously at a flow rate of 20ml/min. Then the freezer was set to -160°C to  
169 cool the sample below the predicted glass transition temperature of about -121°C.  
170 Samples were held for a minimum of 10 minutes below -125°C (Figure 2). The  
171 temperature was measured in the middle of the sample carrier, where cooling is slowest.

172 **(ii) LT warming:** The sample carrier remained inside the freezer but with the liquid nitrogen  
173 supply shut off for slow warming to -95°C. For fast warming to -40°C the sample carrier  
174 was placed outside the freezer at room temperature. For LT reversed warming, first  
175 500ml of a 50%, then a 40% and then a 30% (w/v) CPA solution were pumped in at  
176 20ml/min to decrease the sample CPA concentration. Simultaneously sample solution  
177 was extracted at 20ml/min. The freezer holding temperature was increased from initially  
178 -25°C to -20°C and then -15°C for 30 minutes. Finally, the freezer was set to -10°C and  
179 1L 1xPBS (at 20°C) was added to decrease the sample CPA concentration to 0% (Figure  
180 2).

### 181 **The temperature-concentration curve**

182 For each LT run the temperature/concentration (T/C) curve was determined by measuring the  
183 CPA concentration of the chamber outlet solution and by correlating this value to the sample  
184 temperature reached at the end of the extraction cycle. Thermocouples inserted into the inlet  
185 and outlet tube and inside the sample carrier were used to monitor the temperature. The  
186 refractive index (Digital Refractometer, Cole-Pamer Brix, 45.0 to 95.0%, EW-02941-33) was  
187 used to determine the CPA concentration of the outlet solution based on a previously  
188 established standard curve [40].

### 189 **Filter system**

190 To maintain AELC beads (average diameter (d) =450µm) inside the sample carrier during  
191 CPA extraction and to avoid filter blockage, a plastic tube (5cm length, d=4cm) was covered  
192 from both ends with a 100µm mesh through which the outlet port was introduced. The filter  
193 was placed 1cm away from the opening of the port – where the suction force was highest – to  
194 avoid the filter getting blocked by beads.



## 195 **Avoiding devitrification**

196 To ensure that devitrification during warming was avoided, a finally sample CPA  
197 concentration of 64% (w/v) had to be reached, before the fast cooling process to below -  
198 121°C was started.

## 199 **Differential scanning calorimetry**

200 To establish the liquidus curve of the newly developed CPA solution, differential scanning  
201 calorimetry (DSC) was used to determine the equilibrium melting point of increasing CPA  
202 concentrations. The method has been described previously in detail [32].

## 203 **Statistics**

204 Statistical analyses were performed by Student's *t*-Test using Excel software.

## 205 **Results**

### 206 **CPA development**

#### 207 **(i) Viscosity - candidate CPA combinations**

208 It was predicted that at least 40% (w/v) penetrating CPAs and a maximum total concentration  
209 of 70% (w/v) CPA should be used to obtain sufficient vitrification for large volumes and  
210 slow cooling rates (<10°C/min) from previous feasibility studies [40]. By using the  
211 observational viscosity test at -40°C only four solutions were identified with a similar  
212 viscosity to 70% (w/v) Me<sub>2</sub>SO when comparing (in increments of 10%) combinations of  
213 Me<sub>2</sub>SO, EG and PG with the non-penetrating CPA glucose. All of these solutions contained  
214 at least 40% (w/v) Me<sub>2</sub>SO, but only 10% (w/v) glucose. The viscosity of another eight  
215 solutions was sufficiently reduced for Liquidus Tracking through the substitution of 10%  
216 (w/v) of a penetrating CPA with methanol (Figure 1). Viscosity of CPA solutions of lowest  
217 toxicity were additionally measured with a Bohlin® CVO automated shear rheometer at 20°C  
218 displaying lowest viscosity for 70% (w/v) Me<sub>2</sub>SO with 4.62mPa·s and highest viscosity for  
219 40% Me<sub>2</sub>SO with 20% EG and 10% glucose (w/v) with 6.51mPa·s (Table 1).

220 **(ii) Testing different sugars and sugar combinations**

221 To improve post-warming LT cell survival, non-penetrating sugars were added to Me<sub>2</sub>SO,  
222 which yielded poor AELC viability when used as a single CPA. Viability of AELC,  
223 incubated in 50% (w/v) Me<sub>2</sub>SO, decreased from 90% +/- 2.15 (n=5) to 5.9% +/-3.6 (n=5).  
224 The addition of 10% (w/v) of any sugar (glucose, fructose, raffinose, sucrose, trehalose)  
225 increased cell viability markedly by up to 50% although the final CPA concentration was  
226 increased to 60% (w/v). The combination of glucose with another sugar (5% (w/v) each) did  
227 not significantly increase cell viability (Figure 3).

228 **(iii) Toxicities of low viscous CPA solutions**

229 Glucose was chosen as a CPA additive because it is readily available in large quantities,  
230 inexpensive and is clinically used. In a pre-screening toxicity test, solutions containing  
231 methanol (10% w/v) were generally more toxic to AELC than those without. Methanol was  
232 only well tolerated when the Me<sub>2</sub>SO concentration was equal or less than 30% (w/v) and with  
233 at least 10% (w/v) EG. The toxicity test was repeated in more replicates with the five most  
234 promising solutions. Additionally, these solutions were used to vitrify AELC in a standard  
235 small volume approach (Table 1, Figure 1). Both tests revealed the same order of  
236 performance with highest viability after treatment being obtained with Me<sub>2</sub>SO/EG/glucose at  
237 a ratio of 4:2:1, followed by a combination of Me<sub>2</sub>SO/EG/methanol/glucose at a ratio of  
238 2:3:1:1 (Table 1). EG exhibited lower toxicity to AELC than Me<sub>2</sub>SO and PG when in  
239 combination with Me<sub>2</sub>SO. However, a solution of only EG and glucose (6:1), defined too  
240 viscous for LT (data not included in Table 1), exhibited significantly higher toxicity to AELC  
241 than the combination of EG, glucose and Me<sub>2</sub>SO with 50% versus 68% remaining viability  
242 (n=5 , p<0.01).

243 **(iv) Vitrification properties of low toxic CPA solutions**

244 All five low toxicity solutions (Table 1 – solutions >90% viability (test 1)) vitrified (visual  
245 avoidance of ice formation) at a concentration of 70% (w/v), but only Me<sub>2</sub>SO and a  
246 combination of Me<sub>2</sub>SO/EG/Glucose in a ratio 5:1:1 vitrified (visual absence of ice) at 60%  
247 (w/v) (Figure 1). Those solutions that did not vitrify at 60% (w/v) contained 20% (w/v) or  
248 more EG. It was observed that ice disappearance during warming was slowest for a solution  
249 with Me<sub>2</sub>SO/EG/Glucose in a ratio of 4:2:1 (LTdeg), which was the only one that did not  
250 contain 10% (w/v) methanol. Increasing the overall CPA concentration proportionately to  
251 64% (w/v) was found to be consistent with avoidance of visible ice during warming with  
252 LTdeg.

253 Standard small volume vitrification experiments were performed using the 5 CPA solutions  
254 of lowest toxicity and compared with the outcomes for toxicity testing without cryo-cooling  
255 at 0.5°C. Recoveries of viability after 24h culture for vitrification experiments post thaw were  
256 very low using Me<sub>2</sub>SO alone (around 1%), whilst the best outcomes (53%) were seen with  
257 LTdeg (Table 1, Figure 1). From these range setting experiments, LTdeg was chosen to take  
258 forward into the full LT investigations.

259 **Liquidus Tracking experiments**

260 **(i) Heat transfer measurements**

261 When the first LT runs were carried out, using Me<sub>2</sub>SO as a cryoprotectant, (with a freezer  
262 cooling rate of -1°C/minute and a liquid volume of 450ml), the temperature of the sample  
263 inside the sample carrier was approximately 20°C higher than the temperature of the Me<sub>2</sub>SO  
264 equilibrium melting point and 15°C higher than the predicted target temperature. To increase  
265 the sample cooling rate by improving heat transfer, the freezer temperature was set up to  
266 10°C below the predicted Me<sub>2</sub>SO liquidus curve. Although the CPA concentration inside the  
267 outlet tube and the sample carrier is comparable, the solution inside the insulated outlet tube

268 froze at sub-zero temperatures, as a result of its geometry and the resulting higher cooling  
269 rate. To avoid this, first infusions were carried out by operating the pumps manually, and the  
270 outlet was primed with 50% (w/v) CPA when not in use. This allowed the freezer  
271 temperature to be set on hold at -20°C and to maintain the sample/concentration curve close  
272 to the liquids curve until a concentration of 25% (w/v) CPA at -8°C was reached, before  
273 using inlet and outlet pump simultaneously (Figure 4).

#### 274 (ii) **Machine delivered LT: Me<sub>2</sub>SO alone vs. new CPA solution**

275 Initial LT runs using the pump-driven mixing with a volume of 450ml (including 130ml of  
276 settled beads) using Me<sub>2</sub>SO as a single CPA resulted in no post-warming cell viability. When  
277 the newly developed CPA solution Me<sub>2</sub>SO/EG/Glucose (4:2:1) was used, cell viability was  
278 increased to 40% (+/- 7.7%) (n=3).

#### 279 (iii) **Inhomogeneous “cell per bead” survival**

280 It was noted in preliminary studies by using fluorescence microscopy that some of the beads  
281 contained a high proportion of viable cells, while others contained almost exclusively dead  
282 cells after re-warming from LT. It was assumed that the effect was caused by the temperature  
283 difference within the sample carrier (e.g. colder at the carrier wall, bottom or surface and  
284 warmer at the centre). Viability up to a CPA concentration of 35-40% (w/v), reached at a  
285 temperature of -15°C, remained high and inhomogeneous AELC viability in beads was not  
286 observed. The inlet temperature was therefore maintained at -15°C, while increasing the CPA  
287 concentration from 35 to 64% (w/v), to avoid any potential CPA toxicity effects related to  
288 temperature differences within the system. Nevertheless, strong variations in viabilities  
289 between individual beads were observed. It was suspected that stirring the entire sample  
290 volume was inefficient, resulting in regions of poor CPA mixing and therefore potential ice  
291 nucleation.

292 **(iv) The Liquidus Tracking stirrer**

293 To achieve more homogenous mixing conditions, the original Planer stirrer, designed to hold  
294 larger tissue constructs in the middle of the sample carrier while providing efficient CPA  
295 homogenisation, was replaced with a simple propeller stirrer. By using the new propeller  
296 stirrer, viabilities post LT were significantly improved from 38% +/-11.7 to 77% +/- 4.3 (n=4  
297 +/-SD) and strong variations in viable cell numbers between different individual beads were  
298 no longer observed (Figure 5).

299 **(v) Cell density impacts cell survival**

300 Alginate encapsulated spheroids (AES) of high cell densities ( $15 \times 10^6$  cells/ml of beads) were  
301 less affected by LT treatment with new stirrer than AES of low cell density ( $4 \times 10^6$  cells per  
302 ml/beads) with viabilities of 57% +/-9.7 and 11% +/- 6.9, respectively (n=17, p<0.01). Both  
303 cultures were processed within the same run. Beads of either type were easily distinguished  
304 under the microscope, which made it possible to take images of single beads and determine  
305 the viability using the established FDA/PI method.

306 Although this procedure allowed testing of two populations of beads under exactly the same  
307 conditions, cell number and protein synthesis could not be determined because beads of  
308 different cell densities could not be physically separated. Thus, single run experiments were  
309 carried out with batches of either high or low cell density beads. Again higher cell density  
310 resulted in higher cell numbers, viability, albumin and alpha-fetoprotein production post LT  
311 cooling with respect to the positive control. For cell densities of  $17 \times 10^6$  and  $20 \times 10^6$  cells/ml  
312 of beads viability was 70% and 90%, viable cell numbers were 67% and 96% and albumin  
313 and alpha-fetoprotein release were 48% and 57%, and 80% and 88%, respectively (fraction of  
314 the untreated control after 48 hours of post warming – Figure 6).

## 315 **Discussion**

### 316 **Choice of CPA for LT**

317 We observed here that the pumps and stirrer of the semi-automated Liquidus Tracker are  
318 impaired above a viscosity of approximately 900 mPa·s (Me<sub>2</sub>SO at -40°C). Thus, viscosity  
319 was identified as the first limiting factor for developing a new LT CPA solution. Dimethyl  
320 sulfoxide (Me<sub>2</sub>SO), ethylene glycol (EG) and propylene glycol (PG) were selected as  
321 penetrating CPAs based on their relatively low viscosity and their common use in  
322 vitrification protocols. Only four combinations (in increments of 10%) of Me<sub>2</sub>SO, EG and PG  
323 with 10% (w/v) glucose were of sufficiently low viscosity for our purpose. For this reason,  
324 viscosity was reduced by replacing 10% of a higher viscous penetrating CPA with methanol.

325 Monovalent alcohols are not commonly used in cryopreservation protocols, mostly due to  
326 their known high toxic effects on many biological systems. However, methanol has been used  
327 successfully in fish semen and embryo preservation [24,25,42]. In these applications, the  
328 concentration used was 10% or less, which justified the concentration used here. Although of  
329 general high toxicity, methanol was well tolerated when combined with EG and low amounts  
330 (<=30% w/v) of Me<sub>2</sub>SO and due to its high permeability [5] might be considered useful for  
331 some vitrification protocols.

332 Sugars are generally used to decrease the amount of penetrating CPAs while keeping similar  
333 final CPA concentrations and glass-forming tendencies. When testing different sugars for our  
334 LT CPA solutions, Me<sub>2</sub>SO was not replaced, but instead 10% (w/v) sugar was additionally  
335 included. The type of sugar used in our studies appeared to be irrelevant, which might  
336 suggest a general effect like reduced osmotic stress. It is known that sugars osmotically  
337 reduced the cell volume, and therefore triggering reduced uptake of penetrating CPA, which  
338 leads to less intracellular dehydration through CPAs and also reduced osmotic stress when

339 CPAs are washed out. However, we have previously shown that AELC maintain high  
340 viability after one-step addition and dilution of up to 40% (v/v) Me<sub>2</sub>SO when carried out at  
341 low temperatures [40]. The fact that AELC can support strong osmotic changes and that  
342 toxicity is generally and strongly decreased at low temperatures (osmotic stress has been  
343 suggested to increase at lower temperatures as the difference between transmembrane water  
344 fluxes and movement of penetrating CPA increases [2]) might also indicate additional  
345 effects, such as cell membrane stabilization or even some sort of biochemical toxicity  
346 neutralisation comparable to that reported for reduced toxicity of formamide through the  
347 addition of Me<sub>2</sub>SO [12]. For the semi-automated LT process osmotic stress is even further  
348 reduces as lower concentrated CPA solution is continuously added while being mixed by a  
349 stirrer. However, further work will be needed to assess the relevant importance of osmotic or  
350 chemical toxicities within the overall context of LT.

351 Glucose was chosen for further LT studies for two reasons; firstly because it is clinically  
352 available and inexpensive and for automated LT large CPA volumes are needed and secondly  
353 because glucose has been reported to prevent irreversible binding of Me<sub>2</sub>SO to proteins [8].

354 EG is stated to be the least toxic CPA for hepatocyte vitrification [23,30] but for AELC in  
355 LT, the combination of Me<sub>2</sub>SO (40% w/v) and EG (20% w/v) with 10% (w/v) glucose,  
356 resulted in significantly higher viability than either of the CPAs on its own with 10% (w/v)  
357 glucose. This observation corresponds to previous findings from other authors in  
358 chondrocytes and alginate encapsulated HepG2 and  $\beta$ -TC-cells, which suggest that  
359 combinations of penetrating CPAs are less toxic than the use of a single CPA [20,26,46]. We  
360 could find no explanation for the interaction between EG and Me<sub>2</sub>SO, but both solutions are  
361 also main components of the well-known and commercially available vitrification solutions  
362 VS55 and M22 [12,14]. A similar composition of 22% EG and 18% Me<sub>2</sub>SO and 17.5% for

363 both EG and Me<sub>2</sub>SO have also shown good results for the vitrification of cumulus cells [41]  
364 and equine embryos, respectively [35]. It is interesting, that – although developed to be first  
365 of low viscosity and second of low toxicity – our final chosen LT solution for AELC  
366 resembled those that are already commercially sold for other standard vitrification protocols.  
367 We speculate that viscosity plays an important role in realizing an optimum between CPA  
368 penetration and dehydration.

369 When developing new CPA mixtures, it is necessary to assess toxicity of cryoprotectants at  
370 the concentrations needed to vitrify. To get an estimation of the vitrification properties of the  
371 potential CPA solutions, Me<sub>2</sub>SO and the five CPA solutions of lowest toxicity to AELC were  
372 vitrified in small volumes and CPA solutions (without AELC) and were optically compared  
373 for ice formation. Optical assessment of vitrification is only a semi-quantitative method  
374 compared to other physical measurements such as DSC, but it has been used in other studies  
375 [18,50] as a direct method which can allow multiple conditions to be investigated at the same  
376 time. Whilst all solutions vitrified at 70% (w/v) CPA, only Me<sub>2</sub>SO and the mixture of  
377 Me<sub>2</sub>SO/EG/glucose with a ratio of 5:1:1 vitrified at 60% (w/v) final CPA. One probable  
378 explanation why the other four solutions did not vitrify is the higher concentration of EG and  
379 methanol. EG has been described as a less effective vitrifier than Me<sub>2</sub>SO and PG [3] and  
380 methanol only vitrifies on its own under high pressure [6]. However, methanol seemed to  
381 have increased the rate at which ice melts during the warming phase, which could be  
382 advantageous for decreasing the amount of potential devitrification.

383 The top five low toxicity CPA solutions used to manually vitrify AELC in small volumes  
384 performed generally in the same order as they did in the toxicity studies. Reduced incubation  
385 time before plunging AELC into liquid nitrogen could be beneficial for solutions with higher  
386 concentrations of fast penetrating CPAs (Me<sub>2</sub>SO, methanol), and some solutions might vitrify



387 at lower concentrations which would reduce CPA toxicity and increase viability. For the  
388 chosen set-up the solution of lowest toxicity was superior to the other solutions and proved to  
389 be an efficient vitrifier in the small volume protocol.

390 Final CPA concentrations for LT are of less risk for toxicity than for conventional  
391 vitrification, as they are reached at very low temperatures ( $<-30^{\circ}\text{C}$ ), at which CPA  
392 penetration and toxicity are suspected to be strongly reduced. However, at higher  
393 temperatures CPA toxicity is to be crucial for cell survival during the LT process. This would  
394 point to choosing the lowest toxicity CPA mixture instead of the best vitrifier for AELC  
395 preservation by LT.

#### 396 **The ~~semi-automated~~ machine-delivered LT process**

397 Although LT allows for much slower cooling rates than conventional vitrification, cooling  
398 rates can be still too slow in respect of practicality when large volumes are being cooled. In  
399 our system heat is transferred in two ways: conduction and convection. As the inlet is led  
400 through a tube of several meters that is kept within the freezer chamber, the temperature of  
401 the inlet solution was found to match that of the freezer chamber at the moment of addition.  
402 The shape of the LT sample carrier (small surface area to volume ratio) is unfavourable for  
403 fast cooling and warming rates by conduction. When the temperature difference between the  
404 freezer chamber and sample is small, both conduction and convection have consequently  
405 little impact on the overall sample temperature. Moreover, first CPA addition steps only  
406 require small amounts of highly concentrated CPA solution to increase the sample  
407 concentration. Thus, the initial temperature change by convection can be neglected. For our  
408 work, neither sample volume nor the geometry of the sample carrier could be changed.  
409 However reducing the freezer temperature from  $5^{\circ}\text{C}$  above to  $20^{\circ}\text{C}$  below the predicted  
410 liquidus curve helped to increase the sample cooling rate, although the risk of outlet tube

411 freezing had to be resolved. Using more inlet volume of lower concentrated CPA, thus  
412 increasing convection, can further be used to increase the cooling rate but is logistically more  
413 challenging. This type of approach for LT could be described as semi-automatic; the pumps  
414 had to be operated by manual control to balance the relative volume exchanges as described;  
415 however, the pumps allowed better overall control of solution movement than could be  
416 achieved for example by manual decanting.

417 No viability of AELC was detected when Me<sub>2</sub>SO was used for semi-automated LT, but was  
418 increased to approximately 40% viability when Me<sub>2</sub>SO was replaced with the newly  
419 developed CPA solution, suggesting that CPA toxicity and/or osmotic injury was not fully  
420 suppressed by the LT process. Inhomogeneous distribution of viable and dead cells between  
421 alginate beads led to the assumption that temperature differences within the LT system had  
422 caused this effect. The inlet temperature during the cooling process is much colder than the  
423 sample temperature and there is also a temperature gradient across the sample carrier with  
424 lower temperatures at the outside and higher temperatures on the inside of the sample  
425 container. Inhomogeneous distribution of viable and dead cells was not noted for CPA  
426 concentrations below 35% (w/v), normally reached at -15°C. Consequently, the inlet and  
427 sample solution temperature were maintained at -15°C, thus offsetting the temperature  
428 difference inside the sample carrier, while the sample CPA concentration was increased to  
429 64% (w/v). However, strong variations in the number of viable cells per bead were still  
430 detected, excluding temperature as the main factor for CPA toxicity.

431 Another possibility was that the method of stirring was the cause of this effect. The original  
432 Planer stirrer was designed to operate alongside the sample carrier wall to avoid any  
433 interference with larger, static constructs in the middle of the sample carrier. However, this  
434 design exhibits strong differences across the sample carrier in respect to mixing behaviour.

435 For example, AELC trapped between the static pedals and the moving part of the stirrer are  
436 subject to stronger mixing and higher shear forces than AELC that are located at the centre of  
437 sample carrier. To overcome these mixing differences a propeller stirrer was designed. As a  
438 result viabilities were increased to around 80% and viable and non-viable cells were evenly  
439 distributed across alginate beads. The inlet port being in close proximity to the Planer stirring  
440 system is consistent with the theory that AELC located in the “intense mixing zone” and  
441 close to the inlet of highly concentrated CPA, experienced high intra- and extracellular CPA  
442 concentration differences and an enhanced mass transport across membranes as a result of  
443 high kinetic energy caused by intensive stirring. Thus, chemical toxicity [12], dehydration  
444 and osmotic stress [44] may have been reinforced through vicious mixing with this system,  
445 which were improved by use of the propeller stirrer.

446 An interesting effect was seen when beads of varying cell densities were used for LT. Low  
447 cell density beads tested in the same experiment, and therefore undergoing exactly the same  
448 procedure as did high cell density beads, showed significantly reduced cell survival post  
449 recovery. To measure cell numbers and protein release exclusively, experiments with beads  
450 of the two different cell densities had to be independently repeated, but the outcomes were  
451 the same. 3D cell cultures of higher cell density showed higher post-warming viability, cell  
452 number and protein release. This is in accordance with previous observations: Higher cell  
453 recovery of hepatocyte spheroids in comparison to single cell suspension following  
454 cryopreservation has been reported by Lee and colleagues [27] and vitrification studies with  
455 primary rat hepatocytes by Magalhães have shown better post-cryopreservation viability for  
456 tissue-like culture than for single cells. They concluded that cell-to-cell contact is beneficial  
457 in the maintenance of viability [29]. This might be due to higher cell activity in 3-D cell  
458 cultures [37, 38], which has been linked to higher cell recovery following cryopreservation in

459 single cell suspension [7]. It should be pointed out that the BAL system would require high  
460 cell density (i.e. high total cell numbers) beads for clinical application [43].

461 In respect of shear forces created by the stirrer during LT, it can be expected that higher cell  
462 density is beneficial, as the outer cells may provide protection to those located closer to the  
463 centre. This also applies in respect of excessive dehydration. In 3-dimensional cell constructs,  
464 water diffuses sequentially from one cell to its neighbour. Cells in the surface layer respond  
465 to osmotic changes in the extracellular medium; interior cells respond only to osmotic  
466 changes in cells of surfaces, and thus are exposed to slower rates of dehydration [28]. Shear  
467 stress is also likely to cause cell death by membrane disruption [36] and would account for a  
468 more homogenous distribution of viable and dead cells amongst beads when the propeller  
469 stirrer was used. However, with the current LT set up, shear stress would not seem to be a  
470 major injurious factor.

471 To further improve the LT system, it would be highly advantageous if the intracellular CPA  
472 and water concentration over the LT process could be monitored. For example, if it can be  
473 shown that CPA toxicity is negligible once CPA and water flux are (nearly) reversed and in  
474 the case that this happens within the temperatures range (0 to -40°C) of CPA addition and  
475 reduction, LT protocols could be suitably adapted. The CPA concentration could then be  
476 increased at a higher temperature to ensure intracellular vitrification before cooling the  
477 sample. Once reached, the concentration needed to prevent devitrification during warming  
478 could be manipulated, for example, by using ice blocking agents [49] to minimise the risk of  
479 unwanted ice nucleation.

## 480 **Conclusion**

481 This work has shown that it is possible to use LT to vitrify large volumes of cell therapies  
482 such as AELC in the 3-D format. Further improvements to equipment technology, especially

483 in respect to more automatization are required. An optimized stirring and CPA inlet system,  
484 as well as the use of 3D cultures of higher cell density ( $>20 \times 10^6$  cells/ml beads) may further  
485 increase post-warming viability and performance in the future. In theory, the LT volume  
486 could be further up-scaled by engineering a larger cell chamber with a scaled stirrer system.

#### 487 **Acknowledgement**

488 We also thank Dr. Paul Matejtschuk and Kiran Malik (NIBSC, a Centre of the Health  
489 Protection Agency) for enabling DSC analysis.

#### 490 **Funding**

491 We thank Planer Plc, the Liver Group Charity and the Wellcome Trust for funding this study.

#### 492 **References**

- 493 [1] J.P. Acker, L.E. McGann, The role of cell-cell contact on intracellular ice formation,  
494 1989. 19 (1989) 367–374.
- 495 [2] Y. Agca, J. Liu, J.J. McGrath, a T. Peter, E.S. Critser, J.K. Critser, Membrane  
496 permeability characteristics of metaphase II mouse oocytes at various temperatures in  
497 the presence of Me<sub>2</sub>SO., *Cryobiology*. 36 (1998) 287–300.
- 498 [3] A. Baudot, L. Alger, P. Boutron, Glass-forming tendency in the system water-dimethyl  
499 sulfoxide, *Cryobiology*. 40 (2000) 151–158.
- 500 [4] M. Bokhari, R.J. Carnachan, N.R. Cameron, S.A. Przyborski, Culture of HepG2 liver  
501 cells on three dimensional polystyrene scaffolds enhances cell structure and function  
502 during toxicological challenge, *J. Anat.* 211 (2007) 567–576.
- 503 [5] J.J. Brand, K.R. Diller, Application and theory of algal cryopreservation, *Nov.*  
504 *Hedwigia*. 79 (2004) 175–189.
- 505 [6] M.J.P. Brugmans, W.L. Vos, Competition between vitrification and crystallization of  
506 methanol at high pressure, *J. Chem. Phys.* 103 (1995) 2661–2669.

- 507 [7] J.-S. Cho, S.-H. Chun, S.-J. Lee, I.-H. Kim, D.-I. Kim, Development of cell line  
508 preservation method for research and industry producing useful metabolites by plant  
509 cell culture, *Biotechnol. Bioprocess Eng.* 5 (2000) 372–378.
- 510 [8] P. Clark, G.M. Fahy, A.M. Karow, Factors influencing renal cryopreservation. II.  
511 Toxic effects of three cryoprotectants in combination with three vehicle solutions in  
512 nonfrozen rabbit cortical slices, *Cryobiology.* 21 (1984) 274–284.
- 513 [9] S.M. Coward, C. Legallais, B. David, M. Thomas, Y. Foo, D. Mavri-Damelin, H.J.  
514 Hodgson, C. Selden, Alginate-encapsulated HepG2 cells in a fluidized bed bioreactor  
515 maintain function in human liver failure plasma, *Artif. Organs.* 33 (2009) 1117–1126.
- 516 [10] M.J. Dijkstra-Tiekstra, S. Hazelaar, E. Gkoumassi, M. Weggemans, J. de Wildt-Eggen,  
517 Comparison of cryopreservation bags for hematopoietic progenitor cells using a WBC-  
518 enriched product, *Transfus. Apher. Sci.* 52 (2015) 187–193.
- 519 [11] E. Erro, J. Bundy, I. Massie, S.-A. Chalmers, A. Gautier, S. Gerontas, M. Hoare, P.  
520 Sharratt, S. Choudhury, M. Lubowiecki, I. Llewellyn, C. Legallais, B. Fuller, H.  
521 Hodgson, C. Selden, Bioengineering the liver: scale-up and cool chain delivery of the  
522 liver cell biomass for clinical targeting in a bioartificial liver support system, *Biores.*  
523 *Open Access.* 2 (2013) 1–11.
- 524 [12] G.M. Fahy, C. daMout, L. Tsonev, B. Khirabadi, P. Mehl, H.T. Meryman, Cellular  
525 injury associated with organ cryopreservation: chemical toxicity and cooling injury, in:  
526 J.J. Lemasters, C. Oliver (Eds.), *Cell Biol. Trauma*, CRC Press, Boca Raton, 1995.
- 527 [13] G.M. Fahy, B. Wowk, Principles of cryopreservation by vitrification, *Methods Mol.*  
528 *Biol.* 1257 (2015) 21–82.
- 529 [14] G.M. Fahy, B. Wowk, J. Wu, J. Phan, C. Rasch, A. Chang, E. Zendejas,  
530 Cryopreservation of organs by vitrification: perspectives and recent advances,  
531 *Cryobiology.* 48 (2004) 157–178.

- 532 [15] J. Farrant, Mechanism of Cell Damage During Freezing and Thawing and its  
533 Prevention, *Nature*. 205 (1965) 1284–1287.
- 534 [16] R. Fleck, B. Fuller, Medicines from animal cell cultures, in: 2007.
- 535 [17] K.K. Fleming, A. Hubel, Cryopreservation of hematopoietic and non-hematopoietic  
536 stem cells, *Transfus. Apher. Sci.* 34 (2006) 309–315.
- 537 [18] X. He, E.Y.H. Park, A. Fowler, M.L. Yarmush, M. Toner, Vitrification by ultra-fast  
538 cooling at a low concentration of cryoprotectants in a quartz micro-capillary: A study  
539 using murine embryonic stem cells, *Cryobiology*. 56 (2008) 223–232.
- 540 [19] C.J. Hunt, Studies on cellular structure and ice location in frozen organs and tissues:  
541 The use of freeze-substitution and related techniques, *Cryobiology*. 21 (1984) 385–  
542 402.
- 543 [20] N.M. Jomha, A.D.H. Weiss, J. Fraser Forbes, G.K. Law, J.A.W. Elliott, L.E. McGann,  
544 Cryoprotectant agent toxicity in porcine articular chondrocytes, *Cryobiology*. 61  
545 (2010) 297–302.
- 546 [21] P. Kilbride, G.J. Morris, S. Milne, B. Fuller, J. Skepper, C. Selden, A scale down  
547 process for the development of large volume cryopreservation, *Cryobiology*. 69 (2014)  
548 367–375.
- 549 [22] C. Koshimoto, P. Mazur, Effects of cooling and warming rate to and from -70 degrees  
550 C, and effect of further cooling from -70 to -196 degrees C on the motility of mouse  
551 spermatozoa, *Biol. Reprod.* 66 (2002) 1477–1484.
- 552 [23] L.L. Kuleshova, X.W. Wang, Y.N. Wu, Y. Zhou, H. Yu, Vitrification of encapsulated  
553 hepatocytes with reduced cooling and warming rates, *Cryo Letters*. 25 (2004) 241–  
554 254.
- 555 [24] F. Lahnsteiner, The effect of internal and external cryoprotectants on zebrafish (*Danio*  
556 *rerio*) embryos, *Theriogenology*. 69 (2008) 384–396.

- 557 [25] F. Lahnsteiner, N. Mansour, T. Weismann, The cryopreservation of spermatozoa of the  
558 burbot, *Lota lota* (Gadidae, Teleostei), *Cryobiology*. 45 (2002) 195–203.
- 559 [26] A. Lawson, H. Ahmad, A. Sambanis, Cytotoxicity effects of cryoprotectants as single-  
560 component and cocktail vitrification solutions, *Cryobiology*. 62 (2011) 115–122.
- 561 [27] J.-H. Lee, D.-H. Jung, D.-H. Lee, J.-K. Park, S.-K. Lee, Effect of spheroid aggregation  
562 on susceptibility of primary pig hepatocytes to cryopreservation, *Transplant. Proc.* 44  
563 (2012) 1015–1017.
- 564 [28] R.L. Levin, E.G. Cravalho, C.E. Huggins, Water transport in a cluster of closely  
565 packed erythrocytes at subzero temperatures, *Cryobiology*. 14 (1977) 549–558.
- 566 [29] R. Magalhães, B. Nugraha, S. Pervaiz, H. Yu, L.L. Kuleshova, Influence of cell culture  
567 configuration on the post-cryopreservation viability of primary rat hepatocytes,  
568 *Biomaterials*. 33 (2012) 829–836.
- 569 [30] R. Magalhães, X.W. Wang, S.S. Gouk, K.H. Lee, C.M. Ten, H. Yu, L.L. Kuleshova,  
570 Vitrification successfully preserves hepatocyte spheroids, *Cell Transplant*. 17 (2008)  
571 813–828.
- 572 [31] I. Massie, C. Selden, H. Hodgson, B. Fuller, Cryopreservation of encapsulated liver  
573 spheroids for a bioartificial liver: reducing latent cryoinjury using an ice nucleating  
574 agent, *Tissue Eng. Part C. Methods*. 17 (2011) 765–774.
- 575 [32] I. Massie, C. Selden, H. Hodgson, B. Fuller, Storage temperatures for cold-chain  
576 delivery in cell therapy: a study of alginate-encapsulated liver cell spheroids stored at -  
577 80°C or -170°C for up to 1 year, *Tissue Eng. Part C. Methods*. 19 (2013) 189–195.
- 578 [33] I. Massie, C. Selden, H. Hodgson, B. Fuller, S. Gibbons, G.J. Morris, GMP  
579 Cryopreservation of Large Volumes of Cells for Regenerative Medicine: Active  
580 Control of the Freezing Process., *Tissue Eng. Part C. Methods*. 20 (2014) 1–46.
- 581 [34] J. Matheny, A.M. Karow, O. Carrier, Toxicity of dimethyl sulfoxide and magnesium



582 as a function of temperature, *Eur. J. Pharmacol.* 5 (1969) 209–212.

583 [35] N. Oberstein, M.K. O'Donovan, J.E. Bruemmer, J. Seidel, E.M. Carnevale, E.L.  
584 Squires, Cryopreservation of equine embryos by open pulled straw, cryoloop, or  
585 conventional slow cooling methods, *Theriogenology*. 55 (2001) 607–613.

586 [36] J. Park, Z. Fan, C.X. Deng, Effects of shear stress cultivation on cell membrane  
587 disruption and intracellular calcium concentration in sonoporation of endothelial cells,  
588 *J. Biomech.* 44 (2011) 164–169.

589 [37] D.E. Pegg, The relevance of ice crystal formation for the cryopreservation of tissues  
590 and organs, *Cryobiology*. 60 (2010) S36–S44.

591 [38] D.E. Pegg, L. Wang, D. Vaughan, Cryopreservation of articular cartilage. Part 3: the  
592 liquidus-tracking method, *Cryobiology*. 52 (2006) 360–368.

593 [39] D.E. Pegg, L. Wang, D. Vaughan, C.J. Hunt, Cryopreservation of articular cartilage.  
594 Part 2: mechanisms of cryoinjury, *Cryobiology*. 52 (2006) 347–359.

595 [40] E. Puschmann, C. Selden, S. Butler, B. Fuller, Liquidus tracking: controlled rate  
596 vitrification for the cryopreservation of larger volumes and tissues., *Cryo Letters*. 35  
597 (2014) 345–355.

598 [41] A.M. Saeed, M.J. Escribá, M.A. Silvestre, F. Garcia-Ximénez, Vitrification and rapid-  
599 freezing of cumulus cells from rabbits and pigs, *Theriogenology*. 54 (2000) 1359–  
600 1371.

601 [42] S. Seki, T. Kouya, R. Tsuchiya, D.M. Valdez, B. Jin, C. Koshimoto, M. Kasai, K.  
602 Edashige, Cryobiological properties of immature zebrafish oocytes assessed by their  
603 ability to be fertilized and develop into hatching embryos, *Cryobiology*. 62 (2011) 8–  
604 14.

605 [43] C. Selden, C.W. Spearman, D. Kahn, M. Miller, A. Figaji, E. Erro, J. Bundy, I. Massie,  
606 S.A. Chalmers, H. Arendse, A. Gautier, P. Sharratt, B. Fuller, H. Hodgson, Evaluation

607 of encapsulated liver cell spheroids in a fluidised-bed bioartificial liver for treatment of  
608 ischaemic acute liver failure in pigs in a translational setting, *PLoS One*. 8 (2013).

609 [44] Y.S. Song, S. Moon, L. Hulli, S.K. Hasan, E. Kayaalp, U. Demirci, Microfluidics for  
610 cryopreservation, *Lab Chip*. 9 (2009) 1874–1881.

611 [45] G.N. Stacey, S. Dowall, Cryopreservation of primary animal cell cultures., in:  
612 *Cryopreserv. Free. Protoc.*, 2007: pp. 271–281.

613 [46] C.A. Valdez, O. Abas Mazni, Y. Takahashi, S. Fujikawa, H. Kanagawa, Successful  
614 cryopreservation of mouse blastocysts using a new vitrification solution, *J. Reprod.*  
615 *Fertil.* 96 (1992) 793–802.

616 [47] L. Wang, D.E. Pegg, J. Lorrison, D. Vaughan, P. Rooney, Further work on the  
617 cryopreservation of articular cartilage with particular reference to the liquidus tracking  
618 (LT) method, *Cryobiology*. 55 (2007) 138–147.

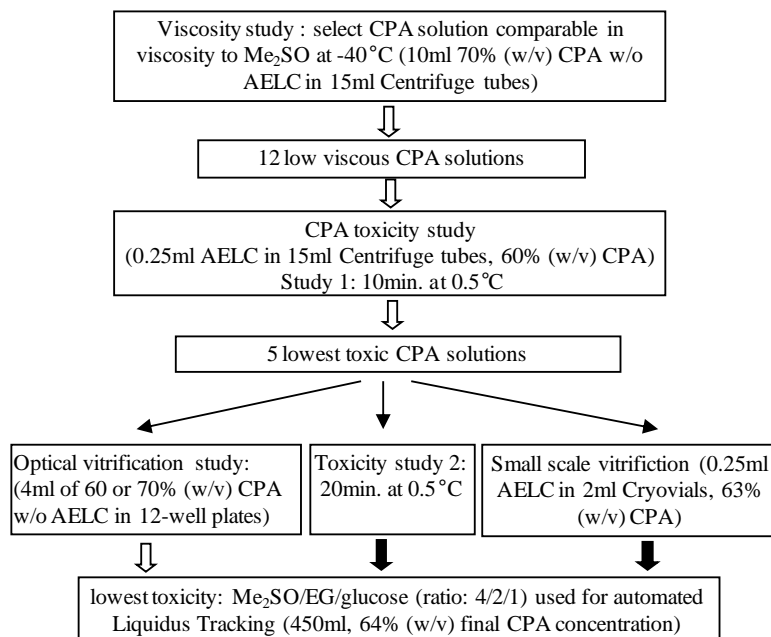
619 [48] W.H. Weihe, The effect of temperature on the action of drugs, *Annu. Rev. Pharmacol.*  
620 13 (1973) 409–425.

621 [49] B. Wowk, E. Leitl, C.M. Rasch, N. Mesbah-Karimi, S.B. Harris, G.M. Fahy,  
622 Vitrification enhancement by synthetic ice blocking agents, *Cryobiology*. 40 (2000)  
623 228–236.

624 [50] B. Wowk, E. Leitl, C.M. Rasch, N. Mesbah-Karimi, S.B. Harris, G.M. Fahy,  
625 Vitrification enhancement by synthetic ice blocking agents, *Cryobiology*. 40 (2000)  
626 228–236.

627  
628  
629  
630  
631

632

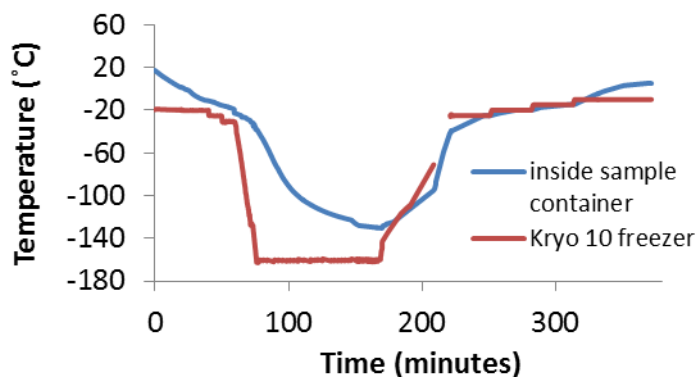


633  
634  
635  
636  
637  
638  
639  
640  
641  
642  
643

**Figure 1: CPA development**

**Step 1:** compare viscosity of combinations of Me<sub>2</sub>SO, EG, PG, glucose (in increments of 10% (w/v)) and methanol (10% (w/v)) to Me<sub>2</sub>SO alone at -40°C. Select combinations with similar viscosity to Me<sub>2</sub>SO. **Step 2:** test toxicity of low viscous CPA solutions on AELC (10 minutes at 0.5°C). **Step 3:** repeat step 3 for 5 lowest toxic CPA solutions for 20 minutes. **Step 4:** test 5 lowest toxic CPA solutions in a standard small scale vitrification process. **Step 6:** visual observation of vitrification properties of 5 low toxic CPA solution. **Step 1-6:** Incubation time and volumes were optimized for each test.

644



645

646

647

**Figure 2: The LT cooling and warming profile**

648

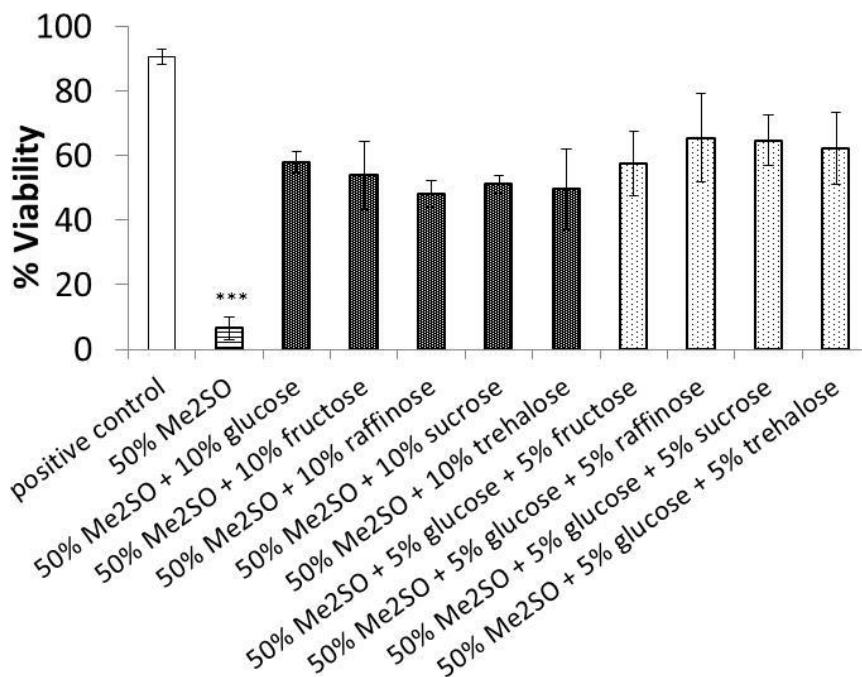
Temperature profile of the LT sample and the freezer were assessed by thermocouples being placed inside the sample (blue line), and inside the freezer chamber (red line). When the sample reached a temperature of  $-95^{\circ}\text{C}$  during warming, the sample container was placed outside the freezer at room temperature (indicated by the interrupted red line at 200 minutes when the chamber was opened) for fast initial warming to achieve a core sample temperature of  $-40^{\circ}\text{C}$ . The freezer chamber temperature was also set at  $-40^{\circ}\text{C}$ , and the sample was returned to the chamber for the reverse LT process. To increase the sample temperature further, the freezer temperature was set manually from initially  $-25^{\circ}\text{C}$  to  $-20^{\circ}\text{C}$  then  $-15^{\circ}\text{C}$  and finally  $-10^{\circ}\text{C}$ , to keep the sample temperature above its liquidus curve and prevent freezing.

656

657

658

659  
660

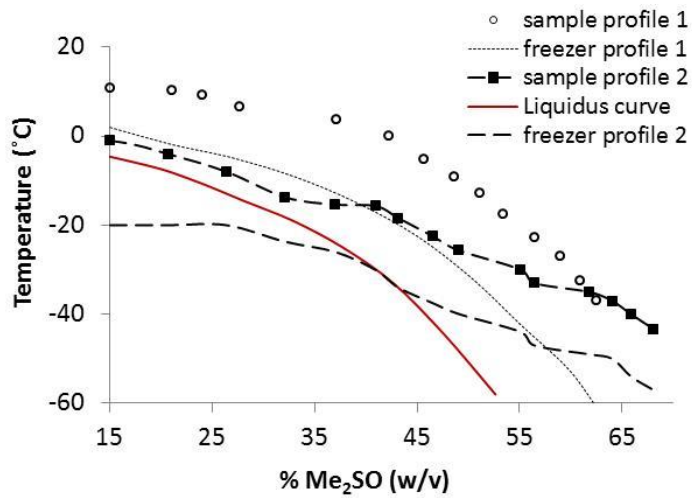


661  
662  
663  
664  
665  
666  
667  
668

**Figure 3: Sugars and sugar combination as non-penetrating CPA — effect in cell viability**

AELC (0.25ml) were incubated in 50% (w/v) Me<sub>2</sub>SO (white) or 50% (w/v) Me<sub>2</sub>SO plus 10% (w/v) sugar, either of one single sugar (grey) or two different sugars (light grey). AELC were incubated for 10 minutes at 0.5°C, using a step-wise CPA addition and reduction procedure. AELC were cultured for 24 hours in complete media at 37°C before measuring viability by FDA/PI staining. Data were n=5 +/- SD. Viability obtained with 50% (w/v) Me<sub>2</sub>SO was significantly lower than with solutions containing sugar, \*\*\*p<0.001.

669



670

671 **Figure 4: Freezer and sample cooling profile relative to the liquidus curve**

672 **Solutions with CPA concentrations below the liquidus curve (red) freeze, while those above remain liquid.**

673 **Liquidus Tracking: by keeping the sample temperature and CPA concentration just above the liquidus**

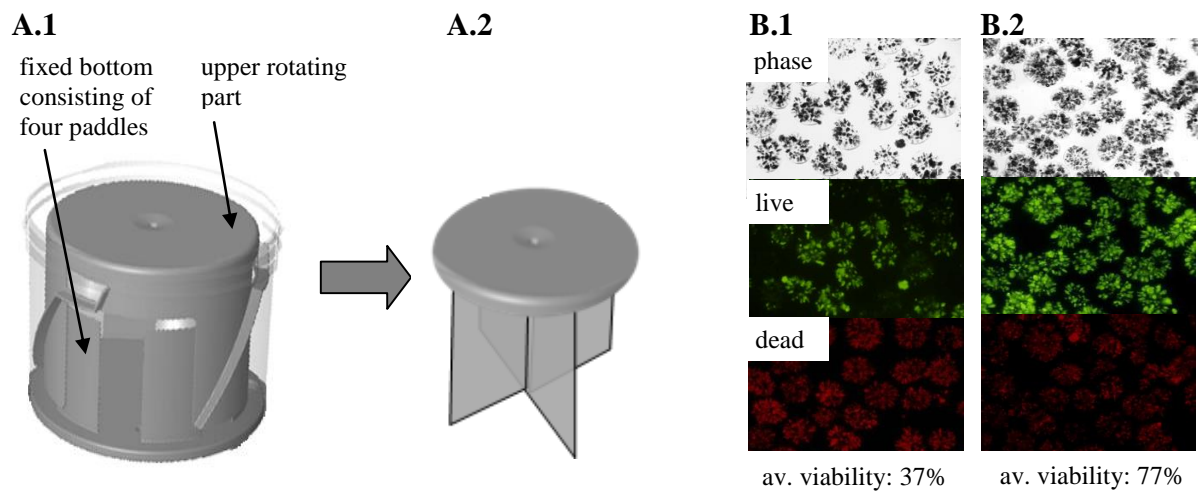
674 **curve, CPA toxicity was reduced and ice nucleation avoided. Freezer cooling profile 1 resulted in a**

675 **discrepancy of ~15°C of the obtained sample profile (profile 1) to the expected profile (not shown) and was**

676 **approximately 20°C higher than the liquidus curve. To increase the sample cooling rate (sample profile 2)**

677 **the freezer temperature (freezer profile 2) was initially set to -20°C below the liquids curve.**

678



679

680 **Figure 5: Planer stirrer versus propeller stirrer**

681 **A1: Planer stirrer — the paddles of the upper part move between the sample carrier wall and the paddles**  
682 **of the bottom part - possibly creating strong differences in mixing behaviour and shear forces between**  
683 **the sample carrier centre and on the outside. A2: Propeller stirrer — used for more homogenous mixing.**  
684 **B1: AELC viability after using the Planer stirrer. B2: Propeller stirrer — viability was significantly**  
685 **increased and bead to bead viability variation was reduced. The figure shows phase images, and images of**  
686 **live (green, stained with FDA) and dead (red, stained with PI) cells.**

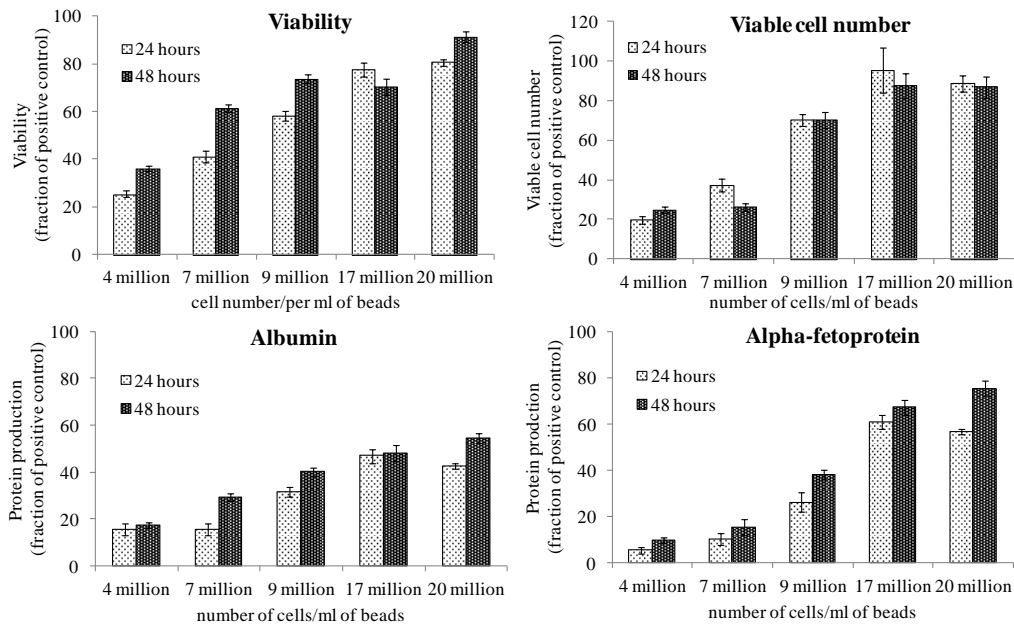
687

688

689

690 **Note: Figure 5- please print in color**

691  
692  
693



694

695 **Figure 6: Impact of low and high cell densities on cell recovery**

696 **The higher the cell density was before the LT process (4, 7, 9, 17, 20 million cells/ml of beads), the higher**  
697 **was the post-warming viability, viable cell number, albumin and alpha-fetoprotein synthesis. For each**  
698 **cell density one LT run was performed. Viability, cell number and protein production were measured in 5**  
699 **replicates for each sample, and shown as means +/- SE . 130ml of beads in 450ml CPA were used.**

700  
701  
702